

Microstructure and crystallographic texture of the chitin–protein network in the biological composite material of the exoskeleton of the lobster *Homarus americanus*

D. Raabe^{a,*}, P. Romano^a, C. Sachs^a, H. Fabritius^a,
A. Al-Sawalmih^a, S.-B. Yi^a, G. Servos^b, H.G. Hartwig^b

^a Max-Planck-Institut für Eisenforschung, Max-Planck-Str. 1, 40237 Düsseldorf, Germany

^b Institut für Morphologische Endokrinologie und Histochemie, Anatomy Department, Düsseldorf University, 40225 Düsseldorf, Germany

Received 1 April 2005; received in revised form 1 August 2005; accepted 1 September 2005

Abstract

The exoskeleton of the lobster *Homarus americanus* is a multiphase biological composite material which consists of an organic matrix (crystalline α -chitin fibers and various types of non-crystalline proteins) and minerals (mainly calcite). In this study we discuss experimental data about the mesoscopic structure and the crystallographic texture (orientation distribution) of the α -chitin–protein fiber network in this material. The synchrotron measurements reveal very strong crystallographic textures of the α -chitin. According to these data, a large fraction of the α -chitin lattice cells is arranged with their longest axis parallel to the normal of the surface of the exoskeleton. Additionally, a smaller fraction of the α -chitin cells is oriented with their longest axis perpendicular to the cuticle surface. These structural investigations reveal the pronounced role of crystallographic orientation distributions in mineralized biological composite materials which may be of relevance for an improved understanding of biological and bio-inspired nano-composites.

© 2006 Published by Elsevier B.V.

Keywords: Crystallographic texture; Microstructure; Microscopy; Plywood structure; Chitin; Nano-composite; Synchrotron; Tissue; Biomineralization; Nanocrystals; Arthropod; Biomaterial

1. Introduction

1.1. The exoskeleton of the American lobster *Homarus americanus*

Lobsters are large arthropods (joint-limb animals), which belong to the class of Crustacea and the order of Decapoda [1,2]. Their body is divided into three main parts: the head (cephalon), the thorax bearing the walking legs, and the tail (abdomen) which ends with the telson. Head and thorax are forming a cephalothorax and the first pair of walking legs evolved into large claws (chelipeds). The slender pincher claw and the bulkier crusher claw differ morphologically according to their function (Fig. 1).

The physical characteristics of decapod crustaceans may vary widely between the different species of this group. The outer covering of these decapods is referred to as exoskeleton or cuticle. It consists – like that of most related crustaceans and the Arthropoda in general – of several layers with specific structural and functional properties. It covers the entire body of the animal and is secreted by a single-layered epithelium. The exoskeleton provides mechanical support to the body, armor against loads that are externally imposed by predators, and enables mobility through the formation of joints and attachment sites for muscles. A functional role also lies in protecting the inner organs from swelling which is essential since the lobster is slightly hyperosmotic to seawater [1,2]. In order to grow, the animals have to replace their old exoskeleton periodically by a new, larger one in a process called molt. Before the old cuticle is shed a new, thin and yet unmineralized cuticle is secreted by the epidermal cells. After the molt the animals grow very quickly and the new soft cuticle is completed and mineralized in order to regain its protective function as fast as possible.

* Corresponding author. Tel.: +49 211 6792 278; fax: +49 211 6792 333.

E-mail addresses: raabe@mpie.de (D. Raabe), romano@mpie.de (P. Romano), sachs@mpie.de (C. Sachs), fabritius@mpie.de (H. Fabritius), sawalmih@mpie.de (A. Al-Sawalmih), yi@mpie.de (S.-B. Yi), hartwig@uni-duesseldorf.de (H.G. Hartwig).

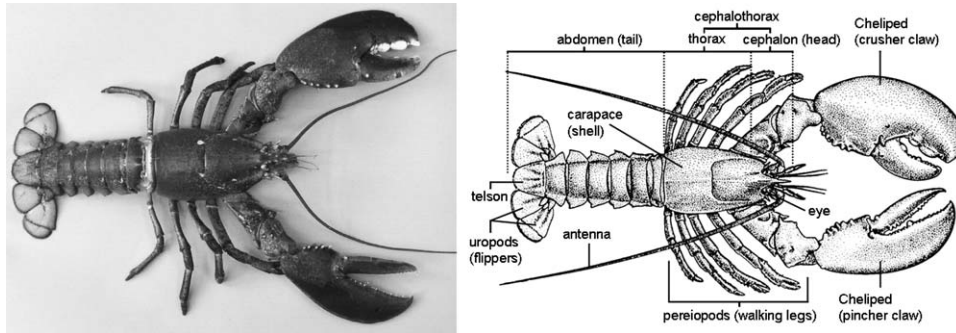


Fig. 1. Dorsal view of *Homarus americanus*. The body length (without antenna) of this specimen was about 0.7 m. The schematic overview depicts the main body parts of the American lobster.

The cuticle is divided in three main layers, referred to as epicuticle, exocuticle, and endocuticle (Fig. 2). A fourth thin membranous layer is present between the three main layers and the epidermal cells during intermolt, the period between two molts. The epicuticle is the outermost layer which is thin and waxy. It consists of long chain hydrocarbons, esters of fatty acids, and alcohols [1–3].

The material of the exo- and the endocuticle is chiefly designed to resist mechanical loads [4–12]. It is a multilayered composite tissue consisting mainly of chitin which is associated with various proteins. In crustaceans, it is usually hardened by considerable amounts of calcium carbonate minerals (typically crystalline calcite and amorphous calcium carbonate) [13–20]. Chitin is a sugar molecule, more specific, an insoluble linear polymer of β -1,4-linked *N*-acetylglucosamine residues. Chitin occurs in three different polymorphic forms that differ in the arrangement of the molecular chains in the crystal cell. α -Chitin is tightly compacted, and the most crystalline polymorphic. In α -chitin, which is the most abundant crystalline variant, the chains are arranged in an anti-parallel fashion. In β -chitin the chains are parallel. It is a crystalline hydrate and water can penetrate between the chains of the β -chitin lattice. γ -Chitin is a mixture of α - and β -chitin with two parallel chains in one direction and the third one in the opposite direction. The three forms can be found in parts of the same organism.

Chitin is the most abundant nitrogen-bearing organic compound in nature and the second most abundant natural polymer on earth after cellulose. Chitin is a common constituent not only of the crustacean cuticle but also of the arthropod exoskeleton in general, including insects, chelicerates, and myriapods. It also occurs in mollusk shells, fungal cell walls, and various other organisms [15,21–25]. The crystalline α -chitin typically predominates in the exoskeleton of large crustaceans.

1.2. Importance of crystallographic texture studies on crustaceans

Mineralized chitin–protein-based nano-scaled composites such as are encountered in the exoskeleton of the lobster *H. americanus* occur in many variants as cuticular materials of arthropods [3–6]. These composites have evolved over a period of 600 million years [1,2]. While the structure and composition of the chitin–protein matrix of the arthropod cuticle [4–12] and the mineralization processes occurring in it [13–20] have received increasing attention, relatively few studies have been carried out on the crystallographic orientation distributions (crystallographic texture) of the α -chitin or of the minerals [28–34]. This applies in particular to the exoskeleton of large crustaceans where no systematic crystallographic texture analysis has been conducted so far.

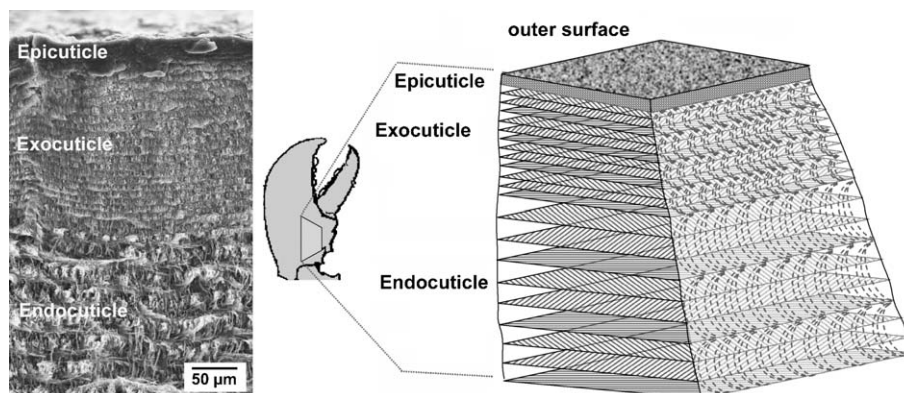


Fig. 2. Scanning electron micrograph (left) of a cross-section through the cuticle and schematic drawing (right) showing the epicuticle, the exo- and the endocuticle of the exoskeleton of the lobster *Homarus americanus*.

Quantitative microstructure and crystallographic texture studies of the exoskeleton of crustaceans (*H. americanus* in this paper) are of relevance for four main reasons.

First, generally a strong relationship exists between the crystallographic and morphological directionality of the microscopic ingredients of biological tissues on one hand and the mechanical and functional anisotropy of these materials on the other [35–37]. When investigating biological matter from an engineering point of view this aspect deserves particular attention since natural constructions seem to exploit the presence of structural anisotropy of its natural constituents in a more efficient and elegant way than most man-made structural materials commonly used in engineering constructions do.

Second, basic crystallographic and orientational issues associated with the nucleation, dissolution, growth, epitaxy, and phase transformation of the minerals in chitin–protein tissue can be tackled on a quantitative basis by the use of modern crystallographic texture analysis [38,39].

Third, texture studies may help towards a better understanding of whether distributions of certain characteristic orientations have evolved following mechanical constructional principles or whether they were developed according to kinetic constraints inherent in the complex biological synthesis of these materials. In other words texture analysis may aid in identifying the prevalence of mechanical versus kinetic building principles behind biological nano-composites.

A fourth and more long-term engineering aspect is the quest to learn more about the basic micromechanical principles that govern the relationship between structure and properties of such nano-composites. This includes a better understanding of the way in which external or internal stimuli support the generation and self-assembly of such intricate though crystallographically highly oriented microstructures. Such effort seems justified for a simple reason: arthropods represent a phylum of invertebrates that includes insects (e.g. beetles, butterflies, ants), crustaceans (e.g. shrimps, crabs, lobsters), and arachnids (e.g. spiders, ticks, scorpions). In terms of their sheer quantity, their evolutionary age, and the variety of niches they occupy, arthropods are very successful animals. More than one million arthropod species have been identified so far—more than 20 times the number of known fish, amphibian, reptile, bird, and mammal species together. Obviously, the material behind the arthropod exoskeleton is a successful natural structural material which, hence, deserves a careful structural analysis from the standpoint of crystallographic texture, substructure, and mechanical properties [4–12]. Therefore, the decapod exoskeleton can serve as an ideal model material to elucidate the structure and properties of arthropod composites owing to the comparatively large sample sizes that can be prepared from it. Such knowledge can also be of help for enhancing corresponding man-made nano-composite concepts relative to their use in the field of medical and constructional engineering [20].

In this study, only a selected range of aspects will be addressed, namely recent results that were obtained on the microstructure and crystallographic texture of the cuticle mate-

rial of the lobster *H. americanus*. The investigation concentrates on the mechanically relevant parts of the exoskeleton (exo- and endocuticle of the hard, mineralized shell).

2. Experimental

2.1. Methods

Samples of the lobster exoskeleton were analyzed by using microscopy and wide angle X-ray diffraction methods. The microstructure was characterized by transmission and reflection light optical microscopy (Leica DM 4000B), scanning electron microscopy (CamScan 4, Zeiss Gemini 1540 XB), and transmission electron microscopy (Hitachi TEM H600). Structure analysis was carried out using a laboratory-scale X-ray diffraction set-up using a Co $K\alpha_1$ beam (Bruker GADDS 5000) and the synchrotron source at ANKA (Angströmquelle Karlsruhe, Germany) [34]. All X-ray sources were operated in conjunction with an area detector using a monochromatic beam in wide angle Bragg diffraction mode for the detection of Debye–Scherrer images. Sets of such diffraction data were used to calculate the pole figures that are needed for the analysis of crystallographic textures and for the identification of different phases [34].

2.2. Sample material and preparation

We used an adult American lobster (*H. americanus*) in intermolt stage acquired from a local seafood supplier. The molting stage was determined by the presence of the basal membrane on the inner surface of the cuticle. Microstructural analysis was conducted on dry specimens which were dissected mainly from the chelipeds. Samples for reflection light optical microscopy were prepared by polishing and gold coating. Samples for transmission light optical microscopy were cut down to 5 μm thickness by using a rotary microtome (Leica RM 2165). Both types of samples were prepared as cross sections with an angular precision below $\pm 5^\circ$. The samples for scanning electron microscopy (SEM) were air-dried and cleaved either perpendicular to the cuticle surface in order to expose the cross-section or parallel to the surface in areas exposing either exo- or endocuticle. The obtained samples were sputter-coated with 5 nm of gold. Samples for transmission electron microscopy (TEM) were fixed with 2.5% glutaraldehyde, decalcified with EDTA, stained and fixed with OsO_4 and uranyl acetate and finally stained with lead citrate to improve contrast before embedding them in Epon resin. Sections of 60 nm thickness were cut using an ultra-microtome. The cuts for the TEM samples were conducted parallel or perpendicular to the surface of the cheliped. Some of the samples were additionally treated with NaOH (5 vol.%) to remove the protein structure. Contrast and brightness of the digital images were adjusted where necessary using Adobe Photoshop CS2 (Adobe Inc., trial version). The samples for the X-ray diffraction experiments were prepared immediately after sacrificing the lobster. Pieces of cuticle from different areas were cut to appropriate sizes using a jewelers saw, washed in 100% methanol, air dried, and stored at -30°C in order to prevent recrystallization of the minerals and natural decaying effects.

3. Results and discussion

3.1. Microstructural hierarchy of the exoskeleton

The tissue of the exo- and the endocuticle of the lobster *H. americanus* consists at the mesoscale (μm -regime) of a complex woven α -chitin–protein fiber network [11,12,40–44], various types of amorphous proteins, and minerals (Fig. 1). Fig. 3a–d shows a set of micrographs of the structure network where all the samples are cross section cuts from the crusher claw. Micrographs in Fig. 3a–c were obtained by optical microscopy and Fig. 3d by transmission electron microscopy (sections of 60 nm thickness).

The micrographs show the twisted plywood-type pattern of the α -chitin–protein fiber network, which is characteristic of the cuticle of arthropods [40–44]. The images reveal two different microstructural scales of the matrix (Fig. 3b–d). In the ensuing discussions, the following definitions will be used in order to distinguish between these two scales: The *thin* helicoidal patterns, which appear in the form of arches due to diagonal cutting in Fig. 3b and c (optical micrographs, cross-section) and Fig. 3d (TEM micrograph, cross-section), are hereafter referred to as *chitin–protein planes*. According to the work of Giraud-Guille [21,24,25,43] and Bouligand [40,42,44] these flat building units are planar arrays of mutually parallel α -chitin–protein fibers. This is supported by the SEM micrographs of lobster cuticle

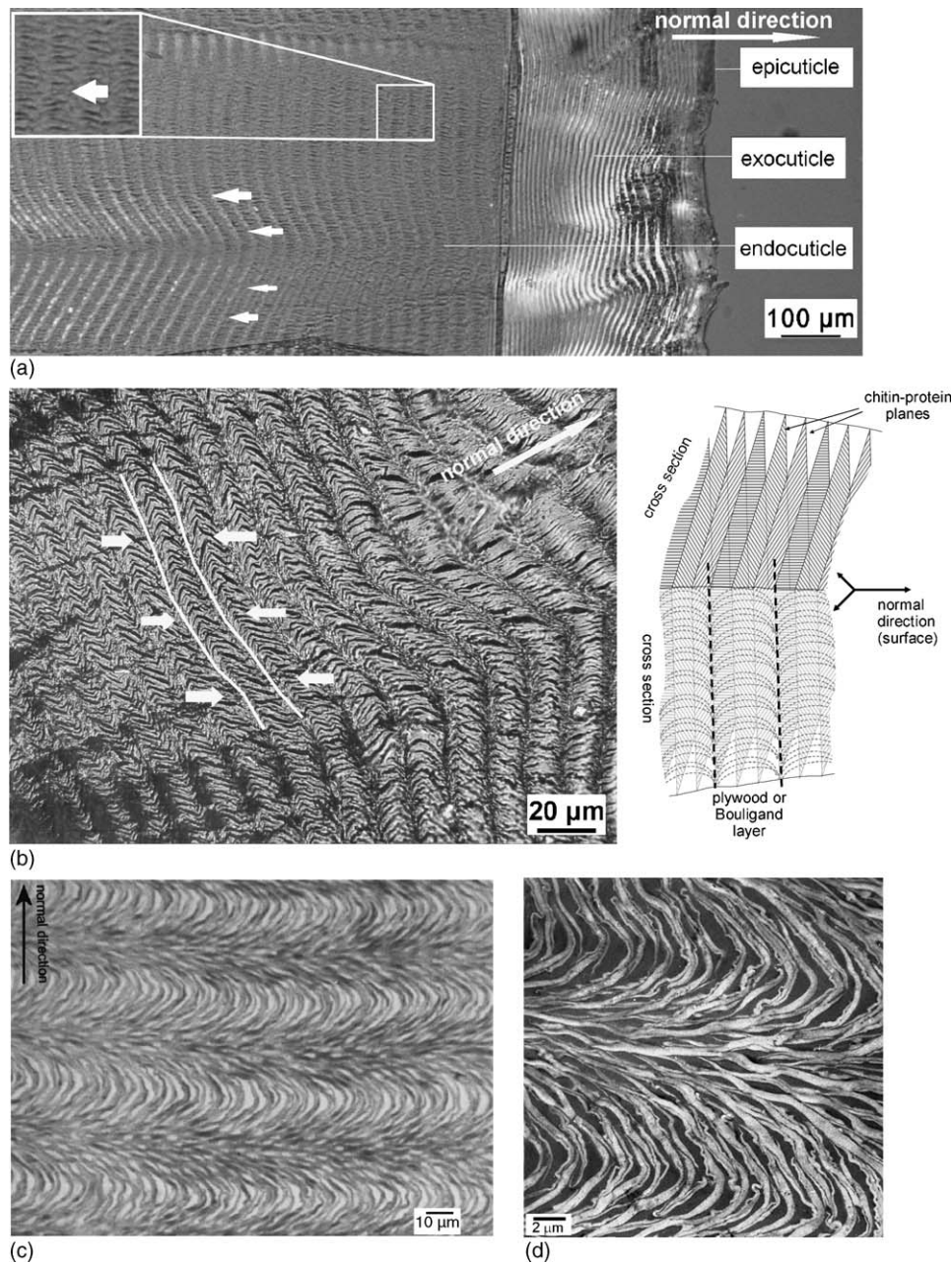


Fig. 3. Cross-sections of the lobster cuticle. Optical micrographs (a–c) of the α -chitin–protein matrix characteristic of the lobster and the arthropod cuticle in general (*Bouligand* or *twisted plywood* pattern) [38–40]. (c) A cross-section prepared for TEM of the structure after removing minerals and proteins. It shows the network of α -chitin–protein fibers. (d) A TEM image of a detail of the network.

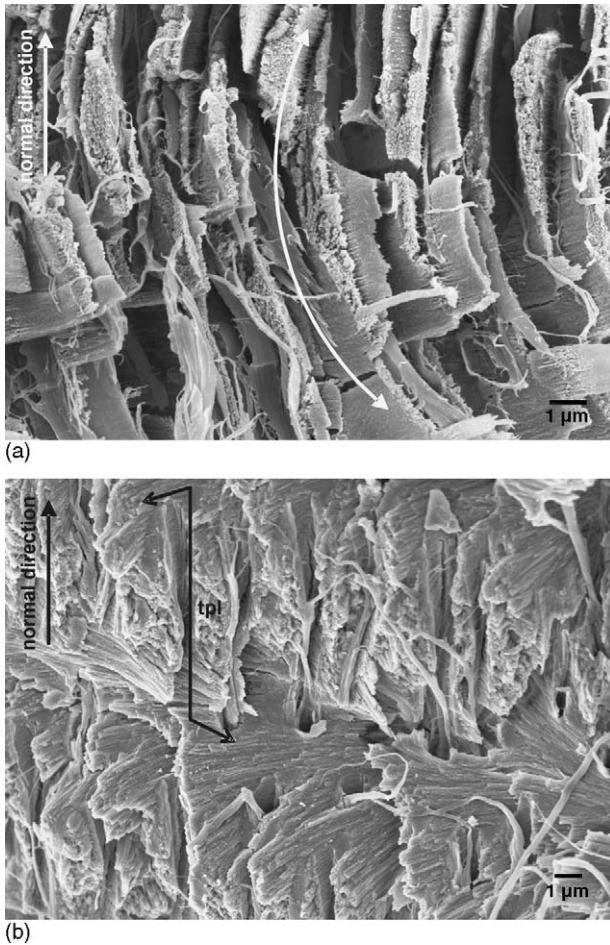


Fig. 4. SEM micrographs of lobster cuticle fractured perpendicular to the surface. (a) The arched pattern (arrow) originates from stacked chitin–protein fibers. (b) Displays stacked twisted plywood layers (tpl) with the chitin–protein fiber planes rotating 180° about the normal direction (indicated by arrows).

fractured perpendicular to the surface (Fig. 4). The fractured surfaces of what appears as arched pattern seen in the optical and TEM micrographs consist of stacked fibers. Their orientation parallel to the cuticle surface gradually rotates along the normal direction (Fig. 4a). The *thick* layers visible particularly in Fig. 3a and b (indicated by white arrows) are bounded by interfaces, which are (when viewed in cross-sections) perpendicular to the arches formed by the chitin–protein planes. These thick layers are hereafter referred to as *Bouligand* or *twisted plywood layers* [40–44]. According to Bouligand [40] they consist of helicoidal stacks of α -chitin–protein planes that are gradually rotated about their normal axis (Figs. 4b and 5). The thickness of the plywood layers corresponds to the stacking height of the α -chitin–protein planes that is required for an accumulated total rotation of 180° about their normal direction (Figs. 3b and 5a). Interfaces appear in the areas where the longitudinal orientation of the chitin–protein fiber planes is parallel to the section plane. This means that small-scale patterning is a building feature inherent in all twisted plywood layers. Fig. 3a and b also show that these layers have a wavy appearance which might be due to some lateral heterogeneity in the synthesis of the underlying α -chitin.

Besides these basic features of the inner structure of the twisted plywood pattern, Fig. 3a also reveals some structural differences between the exo- and the endocuticle. First, the density of the chitin–protein stacks is different in the two regions. This observation was confirmed for different cutting directions. Fig. 3a shows that the exocuticle has a much finer twisted plywood-type mesostructure than the endocuticle. A second observation is that the density of the chitin–protein stacks is not very homogeneous inside the layers. For instance, pronounced variations of the stacking density appear in the exocuticle (Fig. 3a). These lateral variations could be due to local differences in the kinetics during synthesis. Since stereology is important when interpreting micrographs of such composites corresponding sections which were cut parallel to the surface of the lobster claw were also investigated (Fig. 5b–c).

Fig. 5b and c reveal that the helicoidal sequence of the chitin–protein planes corresponds to the commonly assumed model for arthropod cuticles [38–43]. The twisted plywood topography of the layers is characterized by a wide spread of their (topographical) orientation when viewed parallel to the surface. Fig. 5b shows that the structure of the chitin–protein planes in fractured lobster cuticle does not display simple planar layers of parallel fibers as one would expect from earlier literature in that field. They display a morphology resembling the structure of a *peacock feather*. These structures probably originate from the uneven surface of the sample which does not display a single chitin–protein plane but areas where several subsequently rotating planes are cut. Fig. 5c shows many small oblong holes about $2\ \mu\text{m}$ in length dispersed all over the matrix giving the structure a honeycomb like appearance [38]. At higher magnifications it becomes obvious that the holes are lentil shaped cavities left by parallel chitin–protein fibers branching and reconnecting at regular intervals (Fig. 6a and c). Fig. 6b shows that the planes do not rotate stepwise from layer to layer but rather reveal within each plane a smooth gradual rotation of the stacked fibers forming the honeycomb. The holes penetrate the entire structure in a continuous fashion, which is creating the peacock feather-like topological orientation of the chitin–protein fibers in slightly oblique fracture faces [45]. Another interesting feature is the presence of long hose-like structures in the holes of the honeycomb structure (Figs. 4b and 6a and b). Judging from the poor preservation and shrinkage of these structures especially in the samples prepared for SEM, they seem to be of rather soft consistency and thus not mineralized.

High resolution SEM micrographs show that the mineralized α -chitin–protein fiber structure consists of numerous parallel fibrils with diameters of around $20\ \text{nm}$ (Fig. 7a and b). The small fibrils form fibers with diameters between $500\ \text{nm}$ and $2\ \mu\text{m}$. The TEM images (Fig. 7c and d) showing the decalcified chitin–protein fibers in a planar arrangement support this observation. The fibers, which appear in dark gray, have a diameter of about $50\text{--}250\ \text{nm}$ (indicated by white arrows in Fig. 7c). Each of these fibers consists of a bundle of smaller fibrils which in turn consist of parallel crystalline molecule strands (Fig. 7d). This observation of the subdivision of the thick fibers into smaller bundles of fibrils is in accordance with earlier work of Hadley [3], Vincent [4], and Giraud-Guille [24,26] who reported that

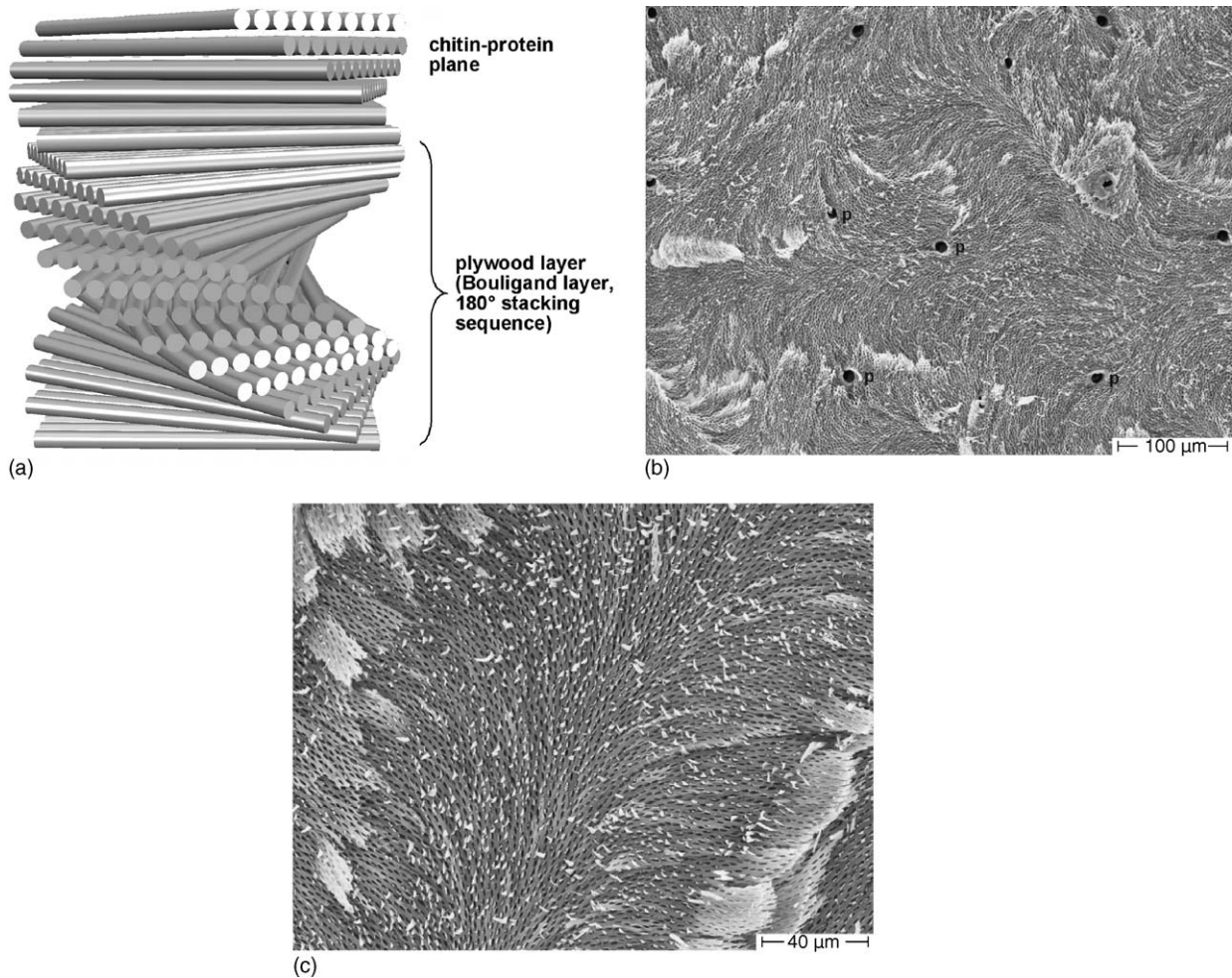


Fig. 5. Schematic (a) and experimental (b, c) images of the helicoidal sequence of the chitin–protein planes within one twisted plywood layer as in-plane view. The SEM micrographs (b) and (c) of endocuticle fractured parallel to the surface show the gradual rotation inherent in the structure. Low magnification (b) reveals an apparently anisotropic topological orientation of the chitin–protein planes which is probably due to the uneven surface of the fractured samples. The holes (p) are cuticular pores. Higher magnifications (c) show that on a smaller scale the arrangement of fibers in obliquely cut chitin–protein planes resembles the structure of a feather.

approximately 18–25 of the polysaccharide molecular chains assemble in narrow and long crystalline units. Proteins are bound to the periphery of these parallel α -chitin fibrils which then aggregate into the thick fibers visible in Figs. 6a, 7a and c [3,21–27].

The overall α -chitin–protein matrix structure reveals a clear network-type arrangement with parallel and branched fibers (Figs. 6 and 7). The branches are indicated by white circles in Fig. 7a and c and indicate where a fiber divides to leave a hole in the honeycomb structure. The branches consist of separate fibers, which regularly connect and disconnect from one another (Fig. 6a and c). Fig. 7d gives a more clear view of the inner structure of the fibers. The small, around 50 nm wide white areas between the fibrils visible in the longitudinally sectioned fibers indicate the presence of some structure which has been removed during preparation of the samples for TEM. The size of these white areas lies in the range of the size of the calcite crystallites incorporated in the lobster cuticle [46]. This is supported by the observation that the fibers in mineralized cuticle from the SEM samples have larger diameters than those in the decalcified

TEM samples. The cross section of the honeycomb holes reveal that their spaces are indeed filled with the hose-like structures observed in the SEM micrographs. The inner structure consists of a (possibly three-dimensional) network consisting probably of proteins. It is conceivable that the role of these hose-like structures could be the transport of calcium and carbonate through the cuticle for hardening it after the molt of the animals. Similar pore canal systems have been described for other species of decapod crustaceans before [47]. They play a role in the transport of calcium ions during the mineralization of the exoskeleton after the molt. Such ion transport systems would be advantageous for large arthropods with thick cuticles where large amounts of mineral have to be deposited in order to harden the cuticle in a relatively short period of time.

3.2. Analysis of the crystallographic texture of the chitin

The analysis of the crystallographic texture of the α -chitin (orthorhombic crystal structure; $a = 4.74 \text{ \AA}$, $b = 18.86 \text{ \AA}$, $c = 10.32 \text{ \AA}$, $\alpha = \beta = \gamma = 90^\circ$) was conducted by measuring sets of

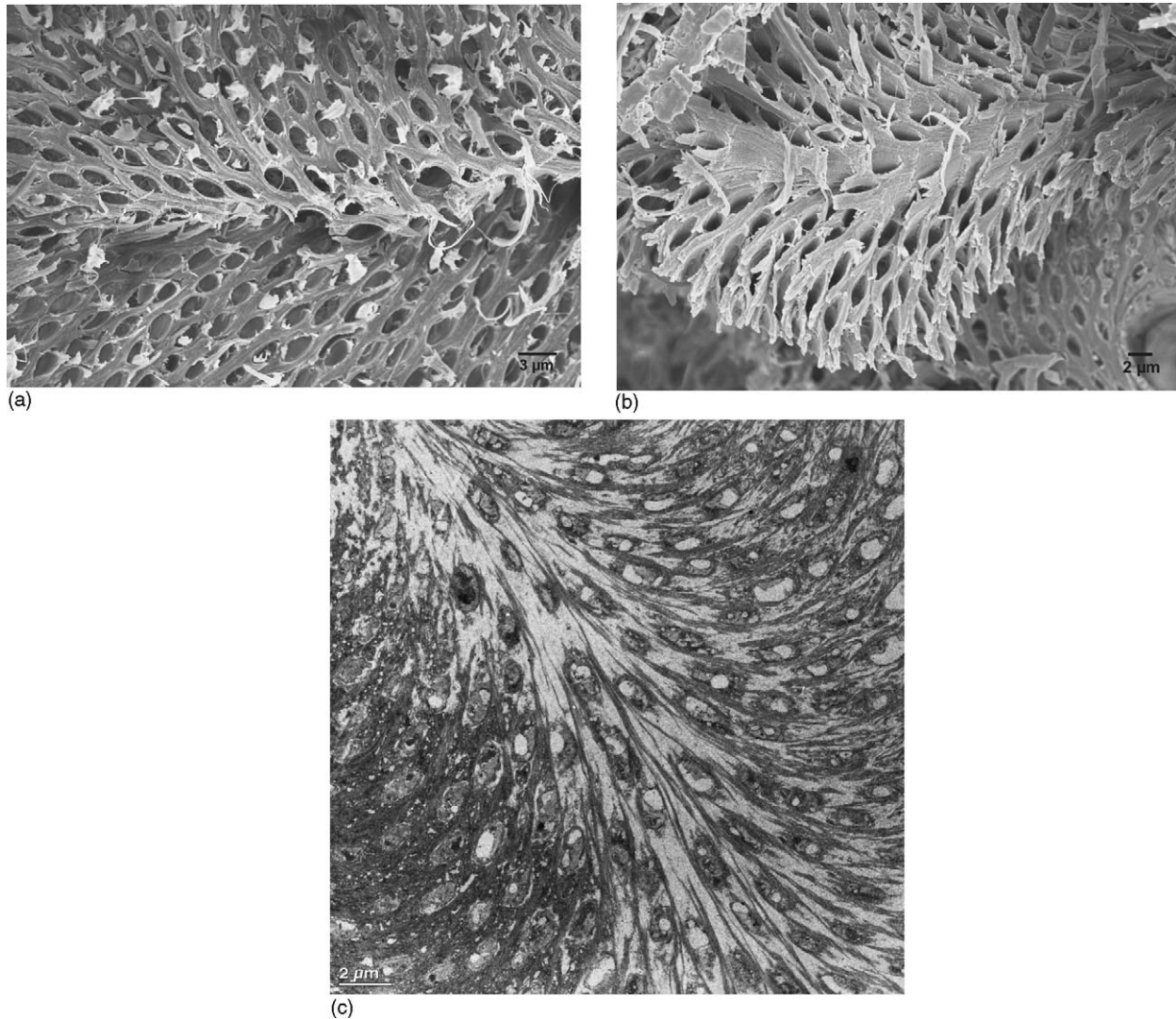


Fig. 6. (a and b) SEM micrographs of the honeycomb-like chitin–protein planes in the endocuticle fractured parallel to the surface of the cuticle. The absence of the hose like structures from a number of holes is due to sample preparation (c) TEM micrograph of the same structure cut from a decalcified portion of the endocuticle. All micrographs reveal small oblong holes about $2\ \mu\text{m}$ long.

Debye–Scherrer images on a sample taken from the left cheliped (claw) of the lobster *H. americanus*. The diffraction data were obtained by using a synchrotron X-ray transmission wide angle set-up in conjunction with an area detector (ANKA synchrotron source in Karlsruhe, Germany) operated at a wavelength of $\lambda = 0.8\ \text{\AA}$.

Corresponding measurements which were alternatively conducted using a laboratory-scale X-ray set-up using Co $K\alpha_1$ radiation with a wavelength of $\lambda = 1.7889\ \text{\AA}$ operated at 40 kV and 40 mA in conjunction with an area detector provided data of slightly weaker pattern quality for texture analysis when compared to the data obtained from the synchrotron measurements.

Fig. 8 shows the crystallographic texture of the α -chitin. The data are presented as three pole figures, (0 2 0), (0 2 1), and (0 0 2) after background correction, normalization, and volume correction. The reference system of coordinates for the projection of the three pole figures is the normal direction of the claw surface (upper direction in pole figure) the longitudinal direction which

is parallel to the axis of the cheliped, and the transverse direction within the cuticle cross-section.

The crystallographic orientation distribution of the chitin–protein network is characterized by various distinct features. First, it reveals a pronounced fiber texture with a very strong crystallographic $\langle 0\ 2\ 0 \rangle$ fiber axis parallel to the surface normal axis of the lobster cuticle (see (0 2 0) pole figure in Fig. 8). This means that a large volume fraction of the α -chitin crystals is oriented in such a way that the long b -axis of their unit cell points towards the surface of the exoskeleton (at least in the claw region from where the sample was taken) (Fig. 9). This observation corresponds to the (0 0 2) pole figure which reveals a strong center fiber in the equatorial plane of the projection matching the 90° orientation relationship between the b -axis and the c -axis of the orthorhombic unit cell. This part of the texture analysis supports the observation of a very strong alignment of the chitin fibers parallel to the surface of the cuticle as also indicated by the micrographs in Figs. 5–7.

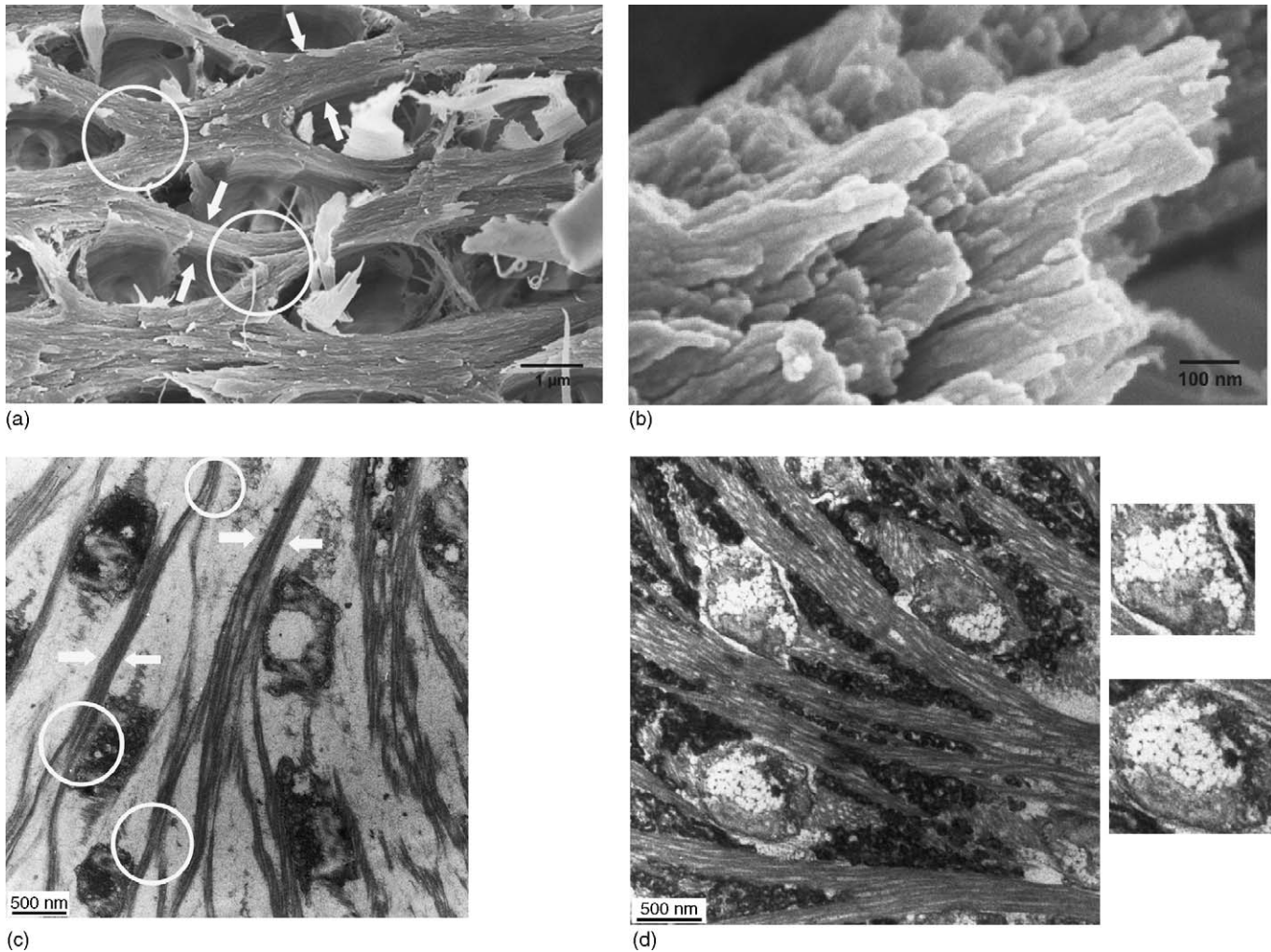


Fig. 7. (a and b) High resolution SEM micrographs showing the architecture of the chitin–protein fibers forming the honeycomb structure. (a) The residues of the soft hose like structures in the pore canals of the honeycomb layers. (c and d) TEM micrographs of the chitin–protein network revealing some inner details of the fibril structure and of the matrix holes. The right hand side of (d) shows some details of the inner structure of the rounded areas. Circles indicate branchings and arrows show the different diameters of the fibers which consist of numerous smaller aggregated fibrils.

Second, another less pronounced crystallographic fiber is visible both, in the (020) and (002) pole figures. It reveals that a second weaker fiber texture exists, which is characterized by the alignment of fibers not only parallel (as in the case of the first strong fiber texture) but also perpendicular to the surface. This conclusion can be drawn from the fact that the crystallographic orientation of the *c*-axis is in the case of the α -chitin crystals strictly equivalent to the topographical orientation of the longitudinal axis of the chitin-fibers. This observation suggests that the chitin–protein network reveals not only a main fiber orientation parallel to the surface but contains also some interpenetrating fibers perpendicular to the surface. The coincidence with the presence of hose-like structures in the pore canals of the honeycomb shaped chitin–protein planes indicates that the walls of these structures are at least partially composed of chitin fibers oriented longitudinally to the long axis of the canals (Figs. 4b, 6a and b, and 7a). Another possibility could be that parts of the fibrous network filling the spaces of the canals consist of chitin (Fig. 7d).

3.3. Reconstruction of the microstructural hierarchy of the exoskeleton of *H. americanus*

The various observations presented above can – enriched by the earlier work in this field quoted in the preceding sections – be summarized as follows. The most characteristic feature of the material is its strictly hierarchical organization which reveals six main different structural levels (Fig. 10).

The first level is the polysaccharide molecule (chitin). The anti-parallel alignment of these molecules leads to α -chitin crystals, which can be regarded as the second level in the hierarchy. The third structural level is the arrangement of 18–25 of the polysaccharide molecular chains in the form of narrow and long crystalline units, which are wrapped by proteins, forming nano-fibrils of about 2–5 nm diameter and about 300 nm length. The fourth level is the clustering of some of these nano-fibrils into long chitin–protein fibers of about 50–250 nm diameter. The fifth level in the hierarchy is the formation of a planar woven and branched network of such chitin–protein fibers. The spacing

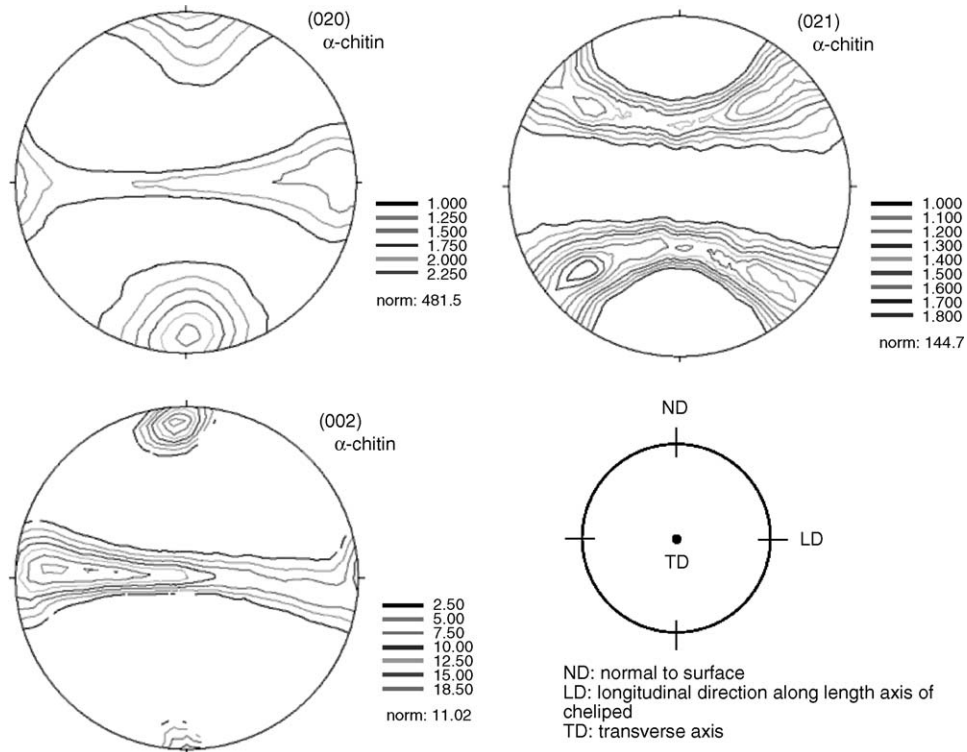


Fig. 8. Pole figures of the α -chitin (orthorhombic crystal structure; $a = 4.74 \text{ \AA}$, $b = 18.86 \text{ \AA}$, $c = 10.32 \text{ \AA}$, $\alpha = \beta = \gamma = 90^\circ$) of a sample taken from the left cheliped of the lobster *Homarus americanus*. The reference system of coordinates for the projection of the two pole figures is the normal direction of the claw surface (upper direction in pole figure) the longitudinal direction which is parallel to the axis of the cheliped, and the transverse direction within the cuticle cross section; $\lambda = 0.196 \text{ \AA}$.

between these strands is filled with a variety of proteins and clusters of minerals (mainly crystalline calcite) which were not investigated in this study. In the case of the lobster, the fibers are arranged in a way that resembles a typical honeycomb with lentil-shaped holes of about $2 \mu\text{m}$ in length which may serve as pore canals. The sixth level, visible already in an optical microscope, is the *twisted plywood* pattern. This level is created from the woven chitin–protein planes which display a feather like

morphology when viewed in samples cut parallel to the surface of the cuticle. The gradual rotation of these planes from one layer to the next creates a rotated honeycomb structure whose pore canals interpenetrate continuously through the entire cuticle. This also leads to mesoscale structures which appear as fiber arches when viewed in cross-sections. The pore canals of the honeycomb structure contain structures which consist at least partly of chitin as revealed by the (0 2 0) and (0 0 2) pole figures.

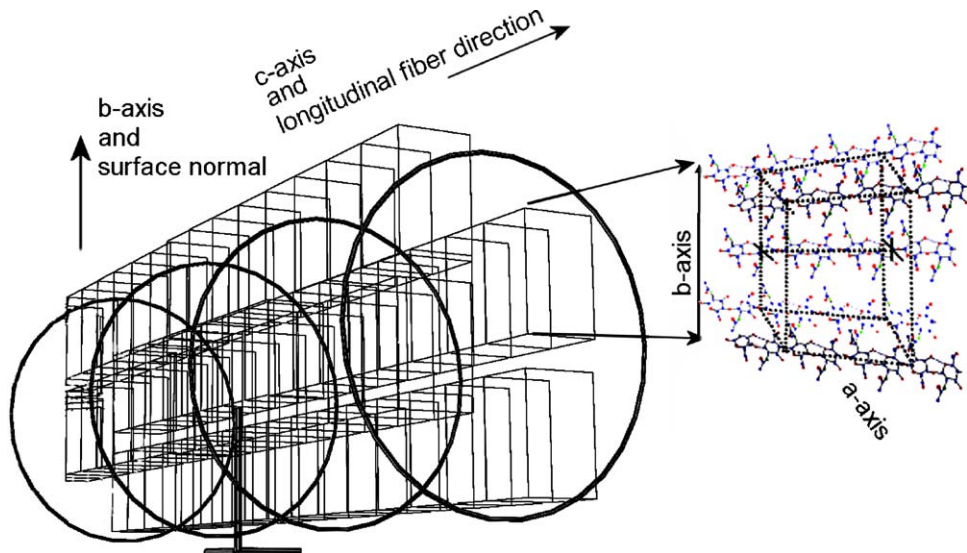


Fig. 9. Schematic representation of the main α -chitin fiber orientation occurring in the (0 2 0) fiber texture of the α -chitin in the claw of the lobster *Homarus americanus*. Letters refer to the lattice cell of the α -chitin with its orthorhombic crystal structure, $a = 4.74 \text{ \AA}$, $b = 18.86 \text{ \AA}$, $c = 10.32 \text{ \AA}$, $\alpha = \beta = \gamma = 90^\circ$.

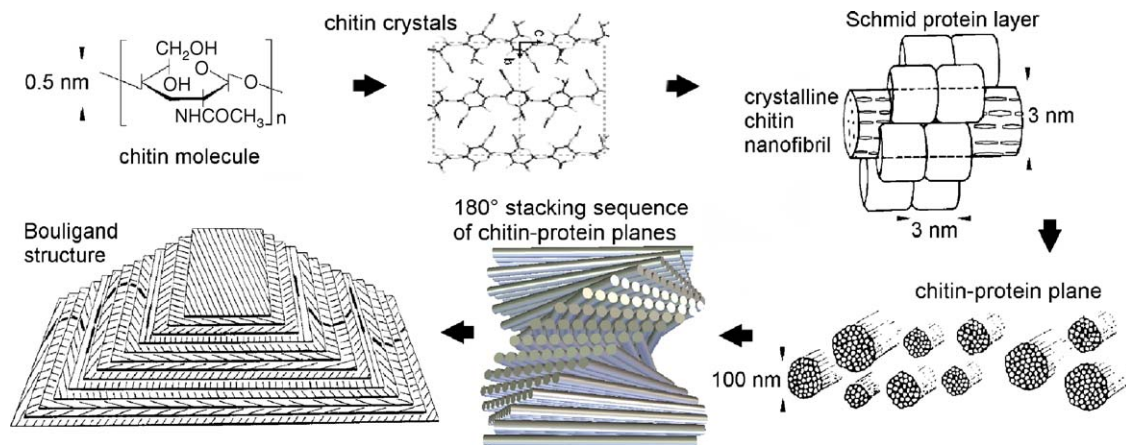


Fig. 10. Hierarchical elements of the twisted plywood structure of the chitin-protein matrix that can be found in the exoskeleton of the lobster *Homarus americanus* [21,24,25].

A stack that rotates 180° around the normal axis is referred to as one Bouligand or twisted plywood layer.

4. Conclusions

We used optical microscopy, electron microscopy, and X-ray wide angle Bragg diffraction for the investigation of the microscopic structure and the crystallographic texture of the exoskeleton of the lobster *H. americanus*. The study reveals a pronounced hierarchical structure of the material and a strong crystallographic texture of the α -chitin-protein network. Our experiments show that the organization of the lobster cuticle is more complex than the commonly assumed model, especially on the level of the twisted plywood structure where it displays a complex honeycombed structure instead of simple planar fibrous layers. The orientation distribution is characterized by a very strong fiber texture with the $\langle 020 \rangle$ fiber axis pointing towards the surface of the cuticle and a less pronounced fiber texture with the $\langle 002 \rangle$ fiber axis pointing perpendicular to the surface of the cuticle. The strong $\langle 020 \rangle$ fiber texture correlates with the arrangement of the chitin on all hierarchical levels observed in the cuticle. The weak $\langle 002 \rangle$ fiber texture results probably from the presence of chitin in the structures that fill the pore canals of the honeycomb, which penetrate the cuticle perpendicularly to its surface.

Acknowledgements

The authors are grateful to the Deutsche Forschungsgemeinschaft (DFG, German Research Foundation) which is funding this study under the framework of the Gottfried Wilhelm Leibniz award. The kind support by the colleagues of the synchrotron source at ANKA (Karlsruhe) is gratefully acknowledged. The authors are grateful to Prof. A. Pyzalla for the synchrotron measurements of the calcite crystallite size.

References

- [1] J. Vernberg, W.B. Vernberg, *The Biology of Crustacea*, Academic Press, New York, USA, 1983.
- [2] M.N. Horst, J.A. Freeman (Eds.), *The Crustacean Integument. Morphology and Biochemistry*, CRC Press, Ann Arbor, Michigan, USA, 1993.
- [3] N.F. Hadley, *Sci. Am.* 255 (1986) 98–106.
- [4] J.F.V. Vincent, *Structural Biomaterials*, Princeton University Press, USA, 1990.
- [5] J.F.V. Vincent, J.D. Currey (Eds.), *Mechanical Properties of Biological Materials*, Society for Experimental Biology, Cambridge, UK, 1980.
- [6] M.F. Ashby, U.G.K. Wegst, *Philos. Mag.* 84 (2004) 2167–2181.
- [7] J.D. Currey, *J. Morphol.* 123 (1967) 1–16.
- [8] J.D. Currey, *Curr. Opin. Solid State Mater. Sci.* 1 (1996) 440–445.
- [9] H.R. Hepburn, I. Joffe, N. Green, K.J. Nelson, *Comp. Biochem. Physiol.* 50 (1975) 551–554.
- [10] C.A. Melnick, S. Chen, J.J. Mecholsky, *J. Mater. Res.* 11 (1996) 2903–2907.
- [11] J.F.V. Vincent, U.G.K. Wegst, *Arthropod Struct. Dev.* 33 (2004) 187–199.
- [12] J.F.V. Vincent, *Composites: Part A* 33 (2002) 1311–1315.
- [13] H.A. Lowenstam, *Science* 211 (1981) 1126–1131.
- [14] S. Mann, J. Webb, R.J.P. Williams, *On Biomineralization*, VCH Press, New York, USA, 1989.
- [15] H.A. Lowenstam, S. Weiner, *On Biomineralization*, Oxford University Press, New York, 1989.
- [16] S. Weiner, L. Addadi, *J. Mater. Chem.* 7 (1997) 689–702.
- [17] S. Mann, *J. Mater. Chem.* 5 (1995) 935.
- [18] F. Manoli, S. Koutsopoulos, E. Dalas, *J. Cryst. Growth* 182 (1997) 116–124.
- [19] G. Falini, S. Albech, S. Weiner, L. Addadi, *Science* 271 (1996) 67.
- [20] M. Epple, *Biomaterialien und Biomineralisation* (in German), Teubner Verlag, Germany, 2003.
- [21] M.-M. Giraud-Guille, Y. Bouligand, in: Z.S. Karnicki, et al. (Eds.), *Crystal Growth in a Chitin Matrix: The Study of Calcite Development in the Crab Cuticle*, Chitin World, Wirtschaftsverlag NW Bremerhaven, 1995, pp. 136–144.
- [22] S.O. Andersen, *Ann. Rev. Entomol.* 24 (1979) 29–61.
- [23] J. Blackwell, M.-A. Weih, *J. Mol. Biol.* 137 (1980) 49–60.
- [24] M.M. Giraud-Guille, *J. Struct. Biol.* 103 (1990) 232–240.
- [25] M.-M. Giraud-Guille, *Tissue Cell* 16 (1984) 75–92.
- [26] S.O. Andersen, *Comp. Biochem. Physiol. Part A* 123 (1999) 203–211.
- [27] Z. Shen, M. Jacobs-Lorena, *J. Mol. Evol.* 48 (1999) 341–347.
- [28] G. Falini, S. Fermani, M. Gazzano, A. Ripamonti, *Chem. Eur. J.* 4 (1998) 1048–1052.
- [29] G. Falini, S. Fermani, A. Ripamonti, *J. Inorg. Biochem.* 84 (2001) 255–258.
- [30] G. Falini, S. Fermani, M. Gazzano, A. Ripamonti, *Chem. Eur. J.* 3 (1997) 1807–1814.
- [31] A.M. Belcher, X.H. Wu, R.J. Christensen, P.K. Hansma, G.D. Stucky, D.E. Morse, *Nature* 381 (1996) 56.

- [32] S. Weiner, Y. Talmon, W. Traub, *Int. J. Biol. Macromol.* 5 (1983) 325.
- [33] M. Iijima, Y. Moriwaki, *Calcif. Tissue Int.* 47 (1990) 237.
- [34] D. Raabe, A. Al-Sawalmih, P. Romano, C. Sachs, H.-G. Brokmeier, S.-B. Yi, G. Servos, H.G. Hartwig, Proceedings of the 14th International Conference on Textures of Materials ICOTOM 14, Leuven, Belgium, Trans Tech Publications, Switzerland, *Mater. Sci. Forum* 495–497 (2005) 1665–1674.
- [35] U.F. Kocks, C.N. Tóme, H.-R. Wenk, *Texture and Anisotropy*, Cambridge University Press, UK, 1998.
- [36] D. Raabe, P. Klose, B. Engl, K.-P. Imlau, F. Friedel, F. Roters, *Adv. Eng. Mater.* 4 (2002) 169–180.
- [37] D. Raabe, F. Roters, F. Barlat, L.-Q. Chen (Eds.), *Continuum Scale Simulation of Engineering Materials*, WILEY-VCH, Weinheim, 2004.
- [38] D. Raabe, P. Romano, C. Sachs, A. Al-Sawalmih, H.-G. Brokmeier, S.-B. Yi, G. Servos, H.G. Hartwig, *J. Cryst. Growth* 283 (2005) 1–7.
- [39] D. Raabe, C. Sachs, P. Romano, *Acta Mater.* 53 (2005) 4281–4292.
- [40] Y. Bouligand, *Tissue Cell* 4 (1972) 189–217.
- [41] S. Hunt, A. El Sherief, *Tissue Cell* 22a (1990) 191–197.
- [42] Y. Bouligand, 7e Congrès, int., *Microsc. Électr.*, vol. 3, Grenoble, France, 1970, pp. 105–106.
- [43] M.-M. Giraud-Guille, *Curr. Opin. Solid State Mater. Sci.* 3 (1998) 221–228.
- [44] Y. Bouligand, in: D. Beysens, N. Boccara, G. Forgacs (Eds.), *Dynamical Phenomena at Interfaces, Surfaces and Membranes*, Les Houches Series, Nova Science Publ. 71–83, 1993.
- [45] A.C. Neville, *Biology of Fibrous Composites*, Cambridge University Press, 1993.
- [46] A. Pyzalla, private communication on synchrotron measurements, 2005.
- [47] D.F. Travis, *Ann. N. Y. Acad. Sci.* 109 (1963) 177–245.